Adsorptive square-wave voltammetry of quasi-reversible electrode processes with a coupled catalytic chemical reaction

Sabrina N. Vettorelo & Fernando Garay

Journal of Solid State Electrochemistry
Current Research and Development in Science and Technology

ISSN 1432-8488

J Solid State Electrochem
DOI 10.1007/s10008-016-3273-9

Springer

J Solid State Electrochem
DOI 10.1007/s10008-016-3273-9

ORIGINAL PAPER

Adsorptive square-wave voltammetry of quasi-reversible electrode processes with a coupled catalytic chemical reaction

Sabrina N. Vettorelo[1] · **Fernando Garay**[1]

Received: 26 March 2016 / Revised: 20 May 2016 / Accepted: 1 June 2016

Abstract There are several strategies for enhancing the sensitivity of electroanalytical methods. Usually, those strategies are based on the selection of the voltammetric technique, the inclusion of an accumulation step, and the eventual addition of a catalytic chemical reaction that regenerates the electroactive species. Square-wave voltammetry (SWV) is one of the most sensitive techniques. In the case of electroanalytical applications, it is typically preceded by an electrochemical or adsorptive pre-concentration step.

In this manuscript, the theory of SWV for a quasi-reversible electrode process coupled to a catalytic chemical reaction between an adsorbed reagent and a soluble product is presented. The dependences of the dimensionless net peak current and its peak potential on the value of the standard charge transfer rate constant are described. The variation of the SWV parameters such as frequency and potential pulse amplitude are discussed. The effect of the chemical and electrochemical kinetics on the voltammetric profile is analyzed.

Keywords Square-wave voltammetry · Catalytic · Mathematical modeling · Adsorption · Quasi-reversible maximum

F. Garay wants to thank to his mentor Prof. Milivoj Lovrić and to Prof. Šebojka Komorsky-Lovrić for all the help and friendship that they gave him since they met. This manuscript is dedicated to them on the occasion of their 65th birthday.

✉ Fernando Garay
fsgaray@gmail.com

[1] INFIQC-CONICET, Departamento de Físico Química, Facultad de Ciencias Químicas, Universidad Nacional de Córdoba, Pabellón Argentina, Ciudad Universitaria, 5000 Córdoba, Argentina

Introduction

Several electroanalytical methods include a pre-concentration step in their potential program. This step usually considers the electrochemical or adsorptive accumulation of electroactive species at the surface of the working electrode [1–10]. Once the electroactive species have been accumulated, the potential is scanned and the current sampled. Square-wave voltammetry (SWV) is one of the most widely employed electrochemical techniques for quantitative analysis. This is because it usually involves fast scans and provides high sensitivity [11–15]. Since the current is sampled at the end of every potential pulse, most of capacitive currents are discarded [11–13]. Besides, the oxidation and reduction pulses of SWV are applied sequentially. As a result, the concentration gradients of reagents and products are enhanced close to the electrode surface and the current is higher than that measured with traditional techniques such as cyclic voltammetry [14, 15].

The net peak current (ΔI_p) is considered to be the most important parameter of SWV since it is used not only for analytical, but also for mechanistic purposes [11–23]. In this regard, the dependences of ΔI_p and the net peak potential (E_p) on the square-wave frequency (f) are essential tools for characterizing the mechanism of a given experimental system [16–23]. Particularly for the case of adsorbed species, the values of ΔI_p can be employed to calculate the charge transfer rate constant (k_s), even for some rather complicated reactions [10, 16–19, 24–26]. Lovrić et al. worked extensively on the theoretical and experimental responses of SWV and especially on those systems where the electrochemical process involves adsorbed species [12, 16–19]. In the case of traces of metal ions, adsorptive accumulation is commonly achieved by adding a suitable ligand that forms a stable and adsorbable complex with the analyte [1–10, 14–19, 27, 28]. The sensitivity of adsorptive stripping voltammetric methods can be

Published online: 09 June 2016

notably increased when they are combined with catalytic reactions [1–10]. This last reaction usually refers to a homogeneous redox reaction in which the reduced form of a metal complex is oxidized back to its initial form, yielding an increase of the reduction current. The sensitivity of a catalytic adsorptive stripping voltammetric method strongly depends on the adsorption constant of the electroactive reagent and the efficiency of the catalytic reaction. The former is controlled by the type of ligand while the latter depends on the kind of reagent chosen for the catalytic step. As a result, it is of particular interest to know the rate constants of the electrochemical step and of the coupled redox reaction.

The theory for a catalytic mechanism of soluble species was developed in 1963 by Smith [29]. However, it was necessary to wait almost 20 years until its first application in SWV [30, 31]. Then, the theoretical model was extended to the cases where redox species are firmly immobilized on the electrode surface [32] and where the catalytic electrode mechanism is coupled to the adsorption equilibria of both redox species [10]. The last case can be considered as an electrode reaction in which the adsorbed forms of the redox couple transfer the electrons while both adsorption equilibria are rapidly compensated from the solution.

In the present work, a theoretical model for the catalytic adsorptive stripping response of SWV is presented. The model considers a quasi-reversible electrode process coupled to a catalytic chemical reaction in which the reagent is adsorbed and the product is released to the solution. The adsorbed reactant is in equilibrium with its soluble part, which is a typical situation found in the adsorptive accumulation of traces of metal ions [1–9].

Mathematical model

The following chemical and electrochemical reactions are analyzed:

$$O_{(sol)} \underset{}{\overset{K_{ad}}{\rightleftarrows}} O_{(ads)} \underset{n}{\overset{k_s}{\rightleftarrows}} R_{(sol)} \tag{1}$$

$$R_{(sol)} + Y_{(ex)} \xrightarrow{k'_{cat}} O_{(sol)} \tag{2}$$

It is assumed that the adsorption of the reactant follows a linear isotherm where the adsorption equilibrium has been achieved and where K_{ad} is the adsorption constant. The electrochemical reaction takes place under conditions of low surface coverage and there are no significant interactions between the adsorbed species. In this regard, the electrode reaction occurs through the adsorbed form of the oxidized species and releases the product in the solution, Eq. (1). The adsorption equilibrium of the oxidized species is reversibly compensated from the solution. Also, the mass transfer has been approximated by the diffusion model of a planar electrode. These simplifications correspond to the adsorptive accumulation of traces of a surface-active electroactive species at a macroelectrode [16–18]. The stripping step corresponds to a cathodic SW scan that takes place in an unstirred solution. The parameter k_s is the charge transfer standard rate constant, and k'_{cat} is the second order forward homogeneous rate constant of the catalytic reaction, Eq. (2). Although the backward rate constant of the catalytic step could be also considered, this assumption would increase the number of variables to study and only irreversible catalytic reactions have been reported [29]. Both equations depend on the 2nd Fick's law according to the following set of differential equations:

$$\partial c_r/\partial t = D\left(\partial^2 c_r/\partial x^2\right) - k_{cat} c_r \tag{3}$$

$$\partial c_o/\partial t = D\left(\partial^2 c_o/\partial x^2\right) + k_{cat} c_r \tag{4}$$

It is assumed a common diffusion coefficient value, $D = 4 \times 10^{-6}$ cm^2 s^{-1}, and that the species Y is in excess, so its concentration is virtually constant in the course of the voltammetric experiment. Therefore, k_{cat} is a pseudo-first order catalytic rate constant defined as $k_{cat} = k'_{cat}\, c^*_y$. Appendix has a list of symbols and abbreviations used in the manuscript. The following boundary conditions are considered for Eqs. (1 and 2):

$$t = 0, \quad x \geq 0: \qquad c_r + c_o = c_o^* \tag{5}$$

$$\Gamma_o^{ini} = K_{ad}\, c_o^* \tag{6}$$

$$c_r = c_r^* = 0 \tag{7}$$

$$t > 0, \quad x \to \infty: \qquad c_o \to c_o^* \tag{8}$$

$$c_r \to 0 \tag{9}$$

$$x = 0: \qquad D(\partial c_o/\partial x)_{x=0} = I/nFA - \partial \Gamma_o/\partial t \tag{10}$$

$$D(\partial c_r/\partial x)_{x=0} = -I/nFA \tag{11}$$

$$I(t)/nFA = k_s \exp[-\alpha\, \varphi(t)] \left\{(c_o)_{x=0} - (c_r)_{x=0} \exp[\varphi(t)]\right\} \tag{12}$$

$$\Gamma_o = K_{ad}(c_o)_{x=0} \tag{13}$$

$$\varphi(t) = nF\left[E(t) - E^{\circ'}\right]/RT \tag{14}$$

where $E(t)$ is the square-wave potential function, $E^{\circ'}$ is the formal potential for a simple redox reaction, n is the number of exchanged electrons, and A is the electrode surface area. The cathodic current has been defined as positive, Eqs. (10–12). Although Eq. (12) is written for soluble species, it does not control the pathway of the electrode reaction. In this regard, the resolution of Eqs. (3 and 4) with the suggested set of boundary conditions determines the functions for the surface concentrations and the way in which the electrode reaction

takes place. Other symbols have their usual meaning. The current is normalized according to:

$$\Psi(t) = I(t)\left[nFAc_o^*(f\pi D)^{1/2}\right]^{-1} \quad (15)$$

where f is the square-wave frequency. The solution of the differential Eqs. 3 and 4 with the relevant boundary conditions is obtained by Laplace transforms. However, before going into the Laplace domain, it is necessary to introduce the following change of variables [29]:

$$\phi = c_r + c_o \quad (16)$$

$$\theta = c_r \exp(k_{cat}t) \quad (17)$$

Thus, a new set of equations is obtained in terms of variables ϕ and θ [29]:

$$\partial\phi/\partial t = D\left(\partial^2\phi/\partial x^2\right) \quad (18)$$

$$\partial\theta/\partial t = D\left(\partial^2\theta/\partial x^2\right) \quad (19)$$

$$D(\partial\phi/\partial x)_{x=0} = -\partial\Gamma_o/\partial t \quad (20)$$

$$D(\partial\theta/\partial x)_{x=0} = -I\exp(k_{cat}t)/nFA \quad (21)$$

The expression for the current is obtained by using the numerical integration method suggested by Nicholson and Olmstead [33]:

$$\Psi_{(m)} = \left\{\lambda - a\xi\,\Xi_{a(m)} - \left[a^2\xi + T_{(m)}\right]\Xi_{b(m)}\right\} \left\{\aleph_{(m)} + a\xi\,\Xi_{a(1)} + \left[a^2\xi + T_{(m)}\right]\Xi_{b(1)}\right\}^{-1} \quad (22)$$

where $\lambda = (f\pi)^{-1/2}$; $\xi = (a^2 - k_{cat})^{-1}$; $\Xi_{a(m)} = \sum_{j=1}^{m-1}\Psi_{(j)}S_{(i)}k_{cat}^{-1/2}$; $\Xi_{b(m)} = \sum_{j=1}^{m-1}\Psi_{(j)}Q_{(i)}$; $a = D^{1/2}(K_{ad})^{-1}$; $T_{(m)} = \exp.[\varphi_{(m)}]$; $\aleph_{(m)} = D^{1/2}k_s^{-1}\exp.[\alpha\,\varphi_{(m)}]$; $S_{(i)} = \mathrm{erf}[(k_{cat}\delta\, i)^{1/2}] - \mathrm{erf}[(k_{cat}\delta(i-1))^{1/2}]$; $i = m - j + 1$; $Q_{(i)} = \exp.[\xi\ \delta\ i]\,\mathrm{erfc}[(k_{cat}\delta\ i)^{1/2}] - \exp.[\xi\ \delta\ (i-1)]\,\mathrm{erfc}[(k_{cat}\delta(i-1))^{1/2}]$; $\delta = (q\,f)^{-1}$ and a value of $q = 50$ was used as the number of subintervals considered for the numerical integration steps. In other words, the variable δ represents a differential of time and each wave was divided in 50 subintervals. This number of time subintervals ensures a numerical error lower than 0.5 % and provides calculated voltammograms within a second [34].

Results and discussion

The studies of the electrode kinetics in SWV can be performed by changing f as well as the square-wave amplitude (E_{sw}). The value of f is usually the parameter of choice since it changes the time scale and, thus, the apparent electrode kinetics of the experiment. Figure 1 shows SW voltammograms calculated for systems with different reversibility of the electrochemical reaction when f is varied from 10 to 1000 Hz. The forward (Ψ_f) and backward (Ψ_b) components of current are indicated in every plot for the sake of clarity. The difference of Ψ_f and Ψ_b gives the dimensionless net current ($\Delta\Psi$). In all cases, the peak of the dimensionless net current ($\Delta\Psi_p$) increases with f. Since the profiles shown in this figure have been calculated for a rather low value of k_{cat}, they are very similar to those described in the pioneering manuscript of Lovrić et al. [16]. Therefore, the value of $\Delta\Psi_p$ depends linearly on the square root of f for systems with irreversible and reversible electrochemical charge transfer. Nevertheless, the dependence of $\Delta\Psi_p$ on f is not linear and shows a maximum. This maximum is a well-known characteristic that is conditioned by the value of k_s and the analyzed timescale [16]. Moreover, the quasi-reversible maximum can be used to estimate the rate of the charge transfer reaction without fitting the experimental data with theoretical curves [18, 35].

In the case of irreversible systems, Ψ_f and Ψ_b have the same sign, Fig. 1A. Besides, the peak potential (E_p) changes linearly with log(f), not shown. For reversible electrochemical reactions, the Ψ_f is higher than Ψ_b, and the ratio between both currents is constant for all frequencies, Fig. 1C. The shape and size of Ψ_f and Ψ_b of quasi-reversible electrochemical systems depend on the timescale of the experiment [16].

Theoretical SW voltammograms corresponding to irreversible, quasi-reversible ,and reversible electrochemical reactions are exhibited in Figs. 2A–C, respectively. On the one hand, the diminution of k_s shifts E_p towards more negative values. On the other hand, SW voltammograms show sigmoid profiles due to the effect of the catalytic reaction. Each of these sigmoid voltammograms is characterized by a respective value of limiting current. The increment of f decreases the magnitude of the dimensionless current because the catalytic reaction has less time to take place. In other words, less amount of product is catalyzed back to the oxidized form of the electroactive species. Since the limiting current of these normalized voltammograms decreases linearly on the square root of f, the dimensional limiting current should be independent of f for systems with high enough values of k_{cat}.

Figure 3 shows the dependence of $\Delta\Psi_p$ as a function of log (k_s) for different values of k_{cat}. Three regions can be observed. It has to be considered that these three regions depend on the timescale of the experiment. All the curves have been calculated at 100 Hz, which is an average value of the available SW frequencies. For k_s >100 cm s^{-1}, the system can be considered as electrochemically reversible and the value of $\Delta\Psi_p$ is a constant that depends on k_{cat}. In a similar way, for k_s <0.01 cm s^{-1}, the system would present an irreversible charge transfer reaction where the value of $\Delta\Psi_p$ is a constant that also depends on k_{cat}. Finally, for 0.01 cm s^{-1} < k_s < 100 cm s^{-1}, the system would be quasi-reversible, and it might exhibit a maximum depending on the value of k_{cat}. The quasi-reversible maximum is observed for systems with relatively low catalytic contribution, curves (a–c).

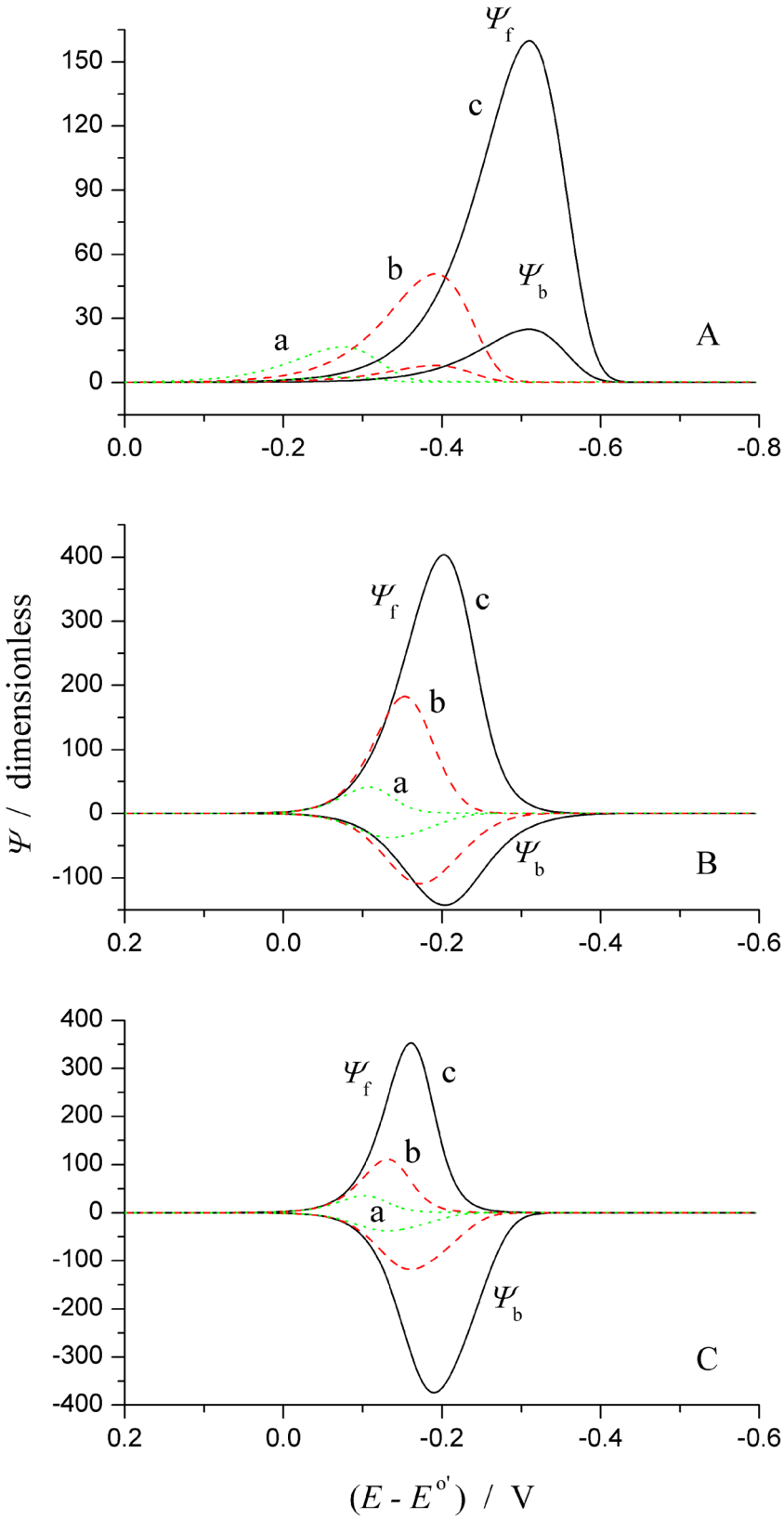

Fig. 1 Theoretical SW voltammograms for $\alpha = 0.5$, $n = 1$, $dE = 5$ mV, $E_{sw} = 50$ mV, $K_{ad} = 0.3$ cm, $k_{cat} = 0.01$ s^{-1}, k_s/cm s^{-1} = (A) 0.001, (B) 1, (C) 1000, f/Hz = (a) 10, (b) 100, and (c) 1000

However, the quasi-reversible maximum disappears for the electrochemical reactions with high values of k_{cat}, curves (d, e).

The effect of E_p on the logarithm of k_s is shown in Fig. 4 for different values of k_{cat}. Again, it is possible to distinguish three

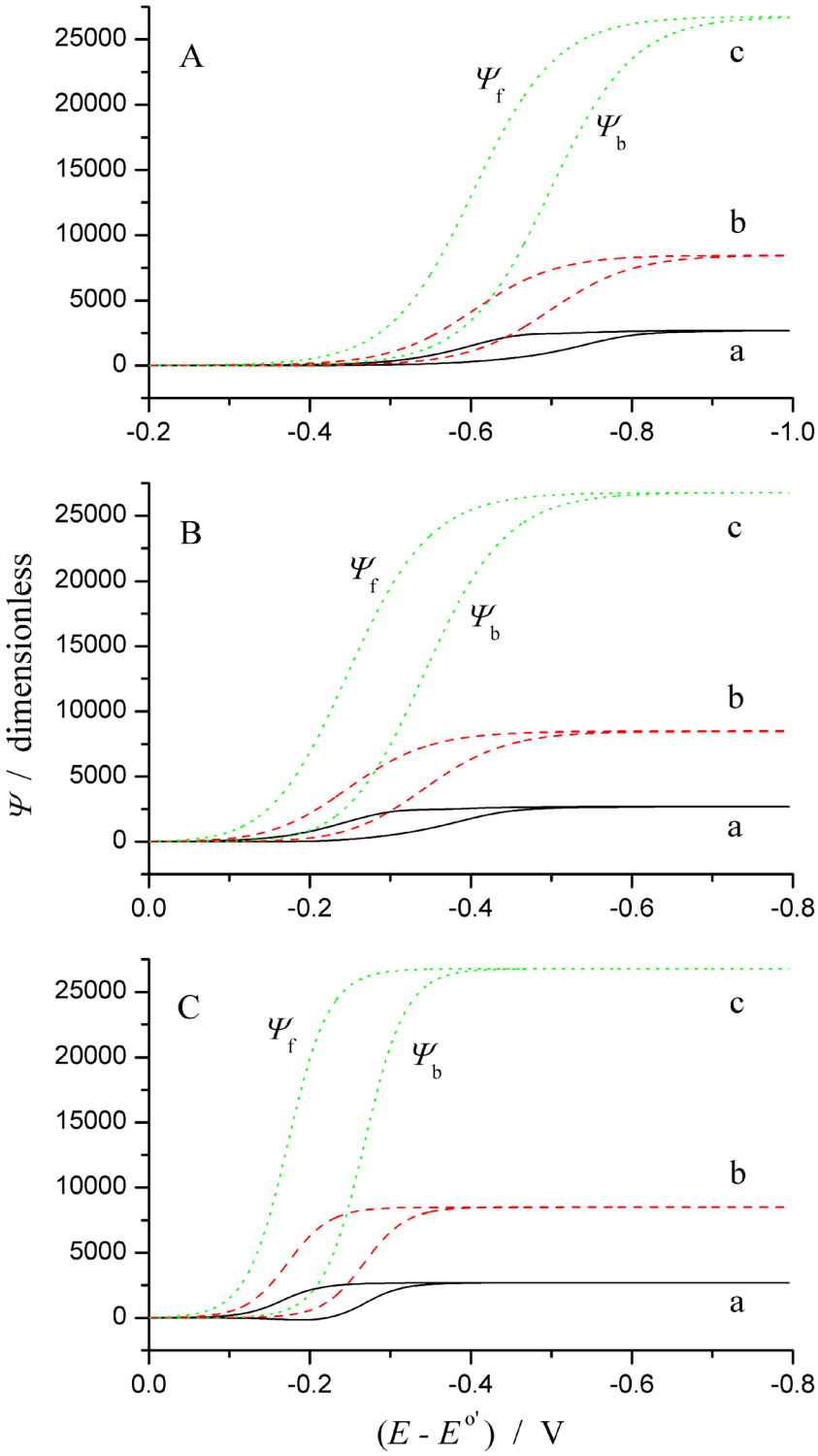

Fig. 2 Calculated SW voltammograms for $\alpha = 0.5$, $n = 1$, $dE = 5$ mV, $E_{sw} = 50$ mV, $K_{ad} = 0.3$ cm, $k_{cat} = 1000$ s^{-1}, k_s/cm s^{-1} = (A) 0.001, (B) 1, and (C) 1000, f/Hz = (a) 10, (b) 100, and (c) 1000

regions. However, the value of k_{cat} affects the range of k_s in which the system behaves as quasi-reversible. For k_{cat} <1 s^{-1} and for k_s >100 cm s^{-1}, the value of E_p is constant and the system can be considered as reversible. Also, for k_{cat} <1 s^{-1} but with k_s <0.01 cm s^{-1}, the value of E_p changes linearly with log (k_s) and has a slope of 0.118 mV dec^{-1}. In both cases, the effect of the catalytic reaction is low. Conversely, the peak potentials depend on both parameters if k_{cat} >1 and k_s <100 cm s^{-1}. When k_{cat} >1 and k_s >100 cm s^{-1}, the value of ;E_p changes linearly with log (k_{cat}) and has a slope of (0.030 ± 0.002) mV dec^{-1}. However, if k_{cat} >1 and k_s <0.01 cm s^{-1}, the value of E_p changes linearly with log (k_{cat}) and has a slope of (0.087 ± 0.003) mV dec^{-1}. For

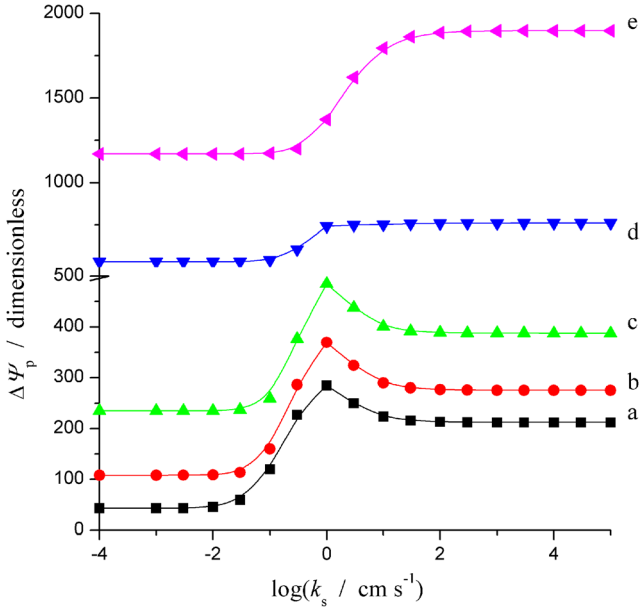

Fig. 3 Dependence of $\Delta\Psi_p$ on the logarithm of k_s calculated for $\alpha = 0.5$, $n = 1$, $dE = 5$ mV, $E_{sw} = 50$ mV, $K_{ad} = 0.3$ cm, $f = 100$ Hz, k_{cat}/s^{-1} = (a) 0.01, (b) 10, (c) 30, (d) 100, and (e) 300

intermediate values of k_s, the system is considered to be quasi-reversible and the value of k_{cat} produces serious changes on E_p. Under those conditions, the dependence of E_p on log (k_s) can change from a constant value to a linear behavior.

Despite the dependencies described above might be of some interest, it is important to take in mind that the kinetic of those systems is controlled by the conditional values of k_s, k_{cat}, and K_{ad}. Thus, the apparent kinetic of those parameters

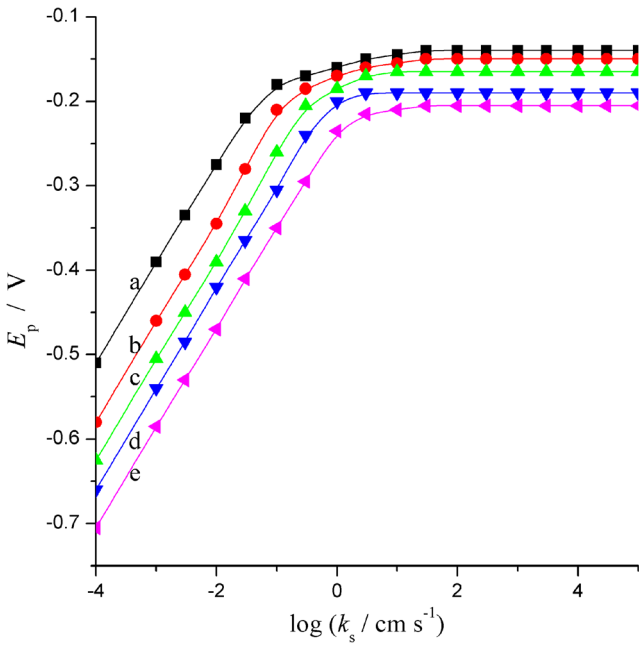

Fig. 4 Dependence of E_p on the logarithm of k_s calculated for $\alpha = 0.5$, $n = 1$, $dE = 5$ mV, $E_{sw} = 50$ mV, $K_{ad} = 0.3$ cm, $f = 100$ Hz, k_{cat}/s^{-1} = (a) 0.01, (b) 10, (e>) 30, (d) 100, and (e) 300

changes and complicates the study when f is varied. Moreover, it becomes practically impossible to find the quasi-reversible maximum of $\Delta\Psi_p$ by varying f. In this regard, it is advisable to modify the concentration of the catalyzer or to vary the value of E_{sw} instead of changing the value of f [32, 36, 37].

As it was stated above, in SWV, the electrode kinetics can be studied also by varying E_{sw}. Figure 5 shows SW voltammograms calculated for a system in which the catalytic and the charge transfer reactions are in the quasi-reversible range. Figure 5A shows SW voltammograms of the normalized net current and Fig. 5B exhibits the forward and backward components of current. The voltammograms of $\Delta\Psi$ show quite symmetric bell-shaped curves for those profiles calculated with the lowest values of E_{sw}. Nevertheless, a slight shoulder appears at potentials more negative than E_p if $E_{sw} < 75$ mV, curves (a, b). For rather high values of E_{sw}, the shoulder separates from the main signal, curves (c, d). The voltammetric peaks can present a second shoulder for scans performed with very high values of E_{sw} and both shoulders appear at potentials more negative than E_p, curves (e, f).

Although in analytical chemistry it is preferred the analysis of the net current, the mechanistic information of electrochemical processes is more evident in Ψ_f and Ψ_b. In this regard, the

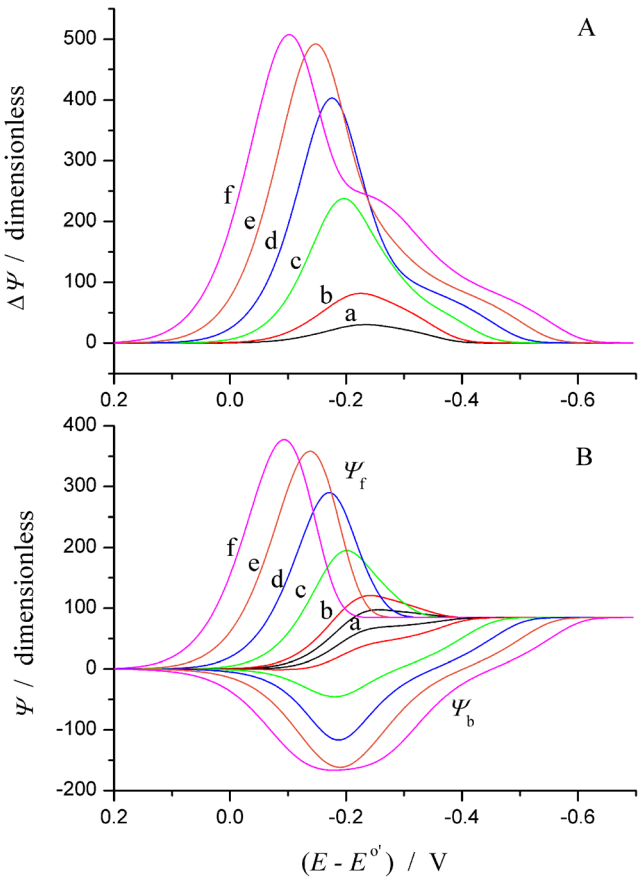

Fig. 5 Theoretical SW voltammograms for $\alpha = 0.5$, $n = 1$, $dE = 5$ mV, $K_{ad} = 0.3$ cm, $k_{cat} = 10\ s^{-1}$, $k_s = 0.1$ cm s^{-1}, $f = 100$ Hz, E_{sw}/mV = (a) 10, (b) 25, (c) 75, (d) 125, (e) 175, (f) 225

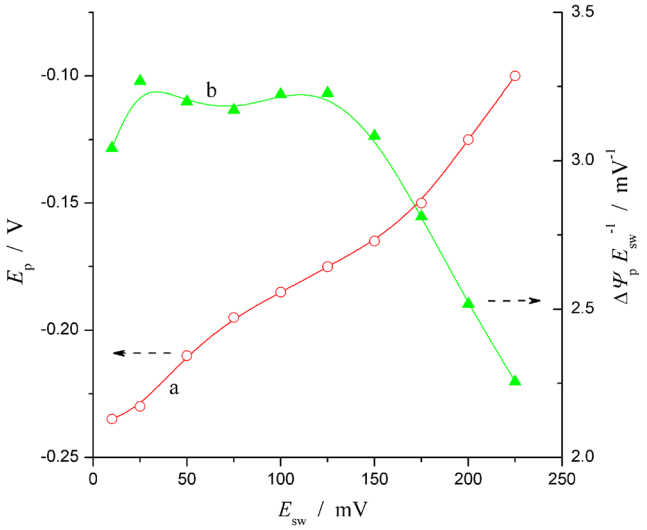

Fig. 6 Dependence of E_p and $\Delta\Psi_p E_{sw}^{-1}$ on E_{sw} calculated for $\alpha = 0.5$, $n = 1$, $dE = 5$ mV, $K_{ad} = 0.3$ cm, $f = 100$ Hz, $k_{cat} = 10\ s^{-1}$, $k_s = 0.1$ cm s^{-1}

forward peaks are quite bell-shaped curves, which are related to the reduction of the adsorbed species. On the contrary, the reduced product is released in solution and has a complex concentration profile. As a result, the function of Ψ_b is also complex. However, the limiting current that is observed at negative potentials is a constant independent of E_{sw}. Although the peak values of Ψ_f and Ψ_b rise with the increment of E_{sw}, they evidence a kind of limiting value. In this regard, above such a limiting value, only the peak width of $\Delta\Psi$ increases. This limiting value depends on the values of k_s and k_{cat}. However, the contribution of both parameters is not simple and requires further analysis.

Figure 6 shows the dependence of E_p and $\Delta\Psi_p E_{sw}^{-1}$ on E_{sw}. As it was indicated above, we are studying if it is possible to extract kinetic information from those curves. The dependence of E_p on E_{sw} exhibits changes on the slope at 25 and at 150 mV. However, the ratio $\Delta\Psi_p E_{sw}^{-1}$ presents maximum values when E_{sw} is close to 25 and 125 mV. Although these dependences might be related to the values of k_s and k_{cat}, it is still unclear the contribution of these parameters to the current. Recently, Mirčeski et al. suggested the use of the maximum value of the ratio $\Delta\Psi_p E_{sw}^{-1}$ for the estimation of k_s [24]. Unfortunately, that relationship cannot be directly applied to the reaction scheme of the present study and further analysis is required.

Conclusion

The theoretical response of SWV for quasi-reversible electrode processes coupled to a catalytic chemical reaction and where the reagent is adsorbed and the product is released to the solution has been presented. The variation of the SW frequency affects the apparent kinetics of the chemical and electrochemical steps. Characteristics such as the quasi-reversible maximum and the linear dependence of $\Delta\Psi_p$ on f for the case of reversible and irreversible systems prevail when $k_{cat} << 1\ s^{-1}$. On the contrary, for the case of $k_{cat} > 10^2\ s^{-1}$, the system is essentially controlled by the catalytic process. For intermediate values of k_{cat}, it is difficult to specify the effect of k_{cat} and k_s from the variation of SW parameters. We are focusing our work on founding one or more simple expressions that help experimentalists to estimate the kinetic parameters of their data.

Acknowledgments Financial support from the Consejo Nacional de Investigaciones Científicas y Tecnológicas (CONICET), Fondo para la Investigación Científica y Tecnológica (FONCYT) and Secretaría de Ciencia y Tecnología de la Universidad Nacional de Córdoba (SECyT-UNC) is gratefully acknowledged. S. V. acknowledges CONICET for the fellowship granted.

Appendix

List of symbols and abbreviations

A	Electrode surface
a	Auxiliary variable of adsorption
c_o	Concentration of oxidized electroactive species
c_o^*	Bulk concentration of oxidized electroactive species
c_r	Concentration of reduced electroactive species
c_r^*	Bulk concentration of reduced electroactive species
D	Diffusion coefficient
δ	Time of a numerical integration step
dE	Potential increment
E_{sw}	Square-wave amplitude
$E(t)$	Dimensioned square-wave potential function
$E^{\circ\prime}$	Formal potential of the redox reaction
E_p	Peak potential
F	Faraday constant
f	Square-wave frequency
Γ_o	Surface concentration of oxidized species
Γ_o^{ini}	Initial surface concentration of oxidized species
$I(t)$	Dimensioned current
ΔI_p	Net peak current
K_{ad}	Adsorption constant
k_s	Standard charge transfer rate constant
k_{cat}	Pseudo-first order catalytic rate constant
k_{cat}	Second order catalytic rate constant
n	Number of exchanged electrons
$\varphi(t)$	Dimensionless potential function
ϕ	Auxiliary concentration function
$\Psi(t)$	Dimensionless current
$\Delta\Psi_p$	Dimensionless net peak current
$\Delta\Psi$	Dimensionless net current
Ψ_b	Dimensionless backward current
Ψ_f	Dimensionless forward current
q	Number of subintervals in each wave
R	Gas constant
T	Temperature in Kelvin degrees
t	Time
θ	Auxiliary concentration function
x	Distance from the electrode surface

References

1. Bobrowski A, Zarebski J (2008) Curr Anal Chem 4:191–201
2. Bănică FG, Ion A (2000) In: Meyers RA (ed) Encyclopaedia of analytical chemistry: instrumentation and applications, vol 12. Wiley, New York, pp. 11115–11143
3. Czae M, Wang J (1999) Talanta 50:921–928
4. Mirčeski V, Bobrowski A, Zarebski J, Spasovski F (2010) Electrochim Acta 55:8696–8703
5. Obata H, van den Berg CMG (2001) Anal Chem 73:2522–2528
6. Caprara S, Laglera LM, Monticelli D (2015) Anal Chem 87:6357–6363
7. Espada-Bellido E, Bi Z, van den Berg CMG (2013) Talanta 105: 287–291
8. Vega M, van den Berg CMG (1997) Anal Chem 69:874–881
9. Abualhaija MM, van den Berg CMG (2014) Mar Chem 164:60–74
10. Mirčeski V, Quentel F (2005) J Electroanal Chem 578:25–35
11. O'Dea JJ, Osteryoung J (1986) In: Bard AJ (ed) Square-wave voltammmetry, electroanal chem, Vol 14, Marcel Dekker, New York, pp 209–308
12. Mirčeski V, Komorsky-Lovrić S, Lovrić M (2007) In: Scholz F (ed) Square-wave voltammertry: theory and application. Heidelberg, Springer Verlag
13. Mirčeski V, Gulaboski R (2014) Maced J Chem Chem Eng 33:1–12
14. Garay F (2001) J Electroanal Chem 505:100–108
15. Garay F (2003) J Electroanal Chem 548:1–9
16. Lovrić M, Komorsky-Lovrić Š (1988) J Electroanal Chem 248:239–253
17. Komorsky-Lovrić Š, Lovrić M (1995) J Electroanal Chem 384: 115–122
18. Lovrić M, Komorsky-Lovrić Š, Bond A (1991) J Electroanal Chem 319:1–18
19. Mirčeski V, Lovrić M (2004) J Electroanal Chem 565:191–202
20. Laborda E, Suwatchara D, Rees NV, Henstridge MC, Molina A, Compton RG (2013) Electrochim Acta 110:772–779
21. Garay F, Lovrić M (2002) J Electroanal Chem 518:91–102
22. Garay F, Lovrić M (2002) Electroanalysis 14:1635–1643
23. Garay F, Lovrić M (2002) J Electroanal Chem 527:85–92
24. Mirčeski V, Laborda E, Guziejewski D, Compton RG (2013) Anal Chem 85:5586–5594
25. Gonzalez J, Molina A, Martinez Ortiz F, Laborda E (2012) J Phys Chem C 116:11206–11215
26. Chevallier FG, Klymenko OV, Jiang L, Jones TGJ, Compton RG (2005) J Electroanal Chem 574:217–237
27. Garay F, Solis VM (2001) J Electroanal Chem 505:109–117
28. Garay F, Solis VM, Lovrić M (1999) J Electroanal Chem 478:17–24
29. Smith DE (1963) Anal Chem 35:602–609
30. O'Dea JJ, Osteryoung J, Osteryoung RA (1981) Anal Chem 53: 695–701
31. Zeng J, Osteryoung RA (1986) Anal Chem 58:2766–2771
32. Mirčeski V, Gulaboski R (2003) J Solid State Electrochem 7:157–165
33. Nicholson RS, Olmstead M (1972) In: Matson J, Mark H, Macdonald H (eds) Electrochemistry: calculations, simulations and instrumentation, Vol 2 Marcel Dekker, New York, pp 120–137
34. Bard AJ, Faulkner LR (2001) In: Electrochemical methods, Wiley, New York, pp 813
35. Garay F, Solis VM (2003) J Electroanal Chem 544:1–11
36. Mirčeski V, Gulaboski R (2015) Electrochim Acta 167:219–225
37. Mirčeski V, Skrzypek S, Ciesielski W, Sokołowski A (2005) J Electroanal Chem 585:97–104